Published in final edited form as:
Reproduction. 2006 April ; 131(4): 771–782. doi:10.1530/rep.1.00870.

Short photoperiod-induced ovarian regression is mediated by apoptosis in Siberian hamsters (*Phodopus sungorus*)

C S Moffatt-Blue, **J J Sury**, and **Kelly A Young**
Department of Biological Sciences, California State University Long Beach, Long Beach, CA 90840, USA

Abstract

Siberian hamster reproduction is mediated by photoperiod-induced changes in gonadal activity. However, little is known about how photoperiod induces cellular changes in ovarian function. We hypothesized that exposing female hamsters to short (inhibitory) as opposed to long (control) photoperiods would induce an apoptosis-mediated disruption of ovarian function. Ovaries and plasma from hamsters exposed to either long (LD, 16 h light:8 h darkness) or short (SD, 8 h light: 16 h darkness) days were collected during diestrus II after 3, 6, 9 and 12 weeks and processed for histology or RIA respectively. Apoptosis was assessed by *in situ* TUNEL and active caspase-3 protein immunolabeling. No significant differences were observed among LD hamsters for any parameter; therefore, these control data were pooled. SD exposure induced a decline in preantral follicles ($P < 0.05$), early antral/antral follicles ($P < 0.01$) and corpora lutea ($P < 0.01$) by week 12 as compared with LD. Terminal atretic follicles appeared by SD week 9; by week 12, these had become the predominant ovarian structures. Estradiol concentrations decreased by weeks 9 and 12 SD when compared with both LD and week-3 SD hamsters ($P < 0.05$); however, no changes were observed for progesterone. TUNEL-positive follicles in SD ovaries increased at week 3 and subsequently declined by week 12 as compared with LD ovaries ($P < 0.01$). Active capsase-3 protein immunostaining peaked at SD week 3 as compared with all other groups ($P < 0.01$). TUNEL and capsase-3 immunolabeling were localized to granulosa cells of late-preantral and early-antral/antral follicles. These data indicate that SD exposure rapidly induces follicular apoptosis in Siberian hamsters, which ultimately disrupts both estradiol secretion and folliculogenesis, resulting in the seasonal loss of ovarian function.

Introduction

To maximize survival when environmental resources are reduced, individuals of many temperate species limit reproductive function seasonally. In mammals, this adaptation is cued primarily by photoperiod-induced alterations in melatonin secretion from the pineal gland. For long-day (LD) seasonal breeders, such as Siberian hamsters (*Phodopus sungorus*), exposure to long photoperiods (>.12.5 h of light per day; short duration of melatonin release) induces and maintains reproductive function, whereas exposure to short photoperiods (<12.5 h of light per day; long duration of melatonin release) results in the cessation of reproductive function (Hoffmann 1986, Bronson 1989, Knopper & Boily 2000, Prendergast & Nelson 2001). Extended periods of melatonin secretion negatively affect reproductive activity via inhibition of the hypothalamic-pituitary-gonadal (HPG) axis. In both males and females, short-day (SD) exposure reduces hypothalamic synthesis and secretion of gonadotropin-releasing hormone (GnRH) and, subsequently, the pituitary gonadotropins, follicle-stimulating hormone (FSH)

Correspondence should be addressed to K A Young; Email: E-mail: kyoung4@csulb.edu.

and luteinizing hormone (LH) (Glass 1986, Buchanan & Yellon 1991). Eventually, these endocrine alterations result in gonadal atrophy or regression, and loss of reproductive function.

The inhibitory effects of short photoperiods on the HPG axis in male Siberian hamsters are well documented (Hoffmann 1979, Bergmann 1987, Furuta *et al.* 1994). Within 6 days of transfer from long to short photoperiods, serum concentrations of both FSH and testosterone are reduced (Yellon & Goldman 1987, Furuta *et al.* 1994). In addition, exposure to (SD) lengths for 6–14 weeks results in significant reduction in testis mass, decline in seminiferous tubule diameter, disruption of spermatogenesis, and alterations in Sertoli and Leydig cell morphology (Bergmann 1987, Young *et al.* 1999). This (SD)-induced testicular regression is mediated in Siberian hamsters and white-footed mice (*Peromyscus leucopus*) by increased apoptotic cell death of germ cells. During regression, incidence of gonadal apoptosis is inversely proportional to declines in testis mass, and components of the apoptotic pathway are upregulated within 3 weeks of short photoperiod exposure in Siberian hamsters (Furuta *et al.* 1994), and within 4–6 weeks in white-footed-mice (Young *et al.* 1999). Conversely, angiogenic factors are downregulated during testicular regression induced by short days in white-footed mice (Young & Nelson 2000, Pyter *et al.* 2005), indicating that expression of a number of gene families may contribute to tissue transformation during gonadal regression.

While the pathways mediating testicular regression have been examined thoroughly, less is known about mediation of seasonal changes in ovarian function. Exposure of female Siberian hamsters to short photoperiod induces loss of estrous cyclicity, declines in plasma FSH concentrations, uterine atrophy, impaired folliculogenesis and, consequently, cessation of ovulation (Schlatt *et al.* 1993). Despite these data, the cellular and molecular mechanisms mediating the reduction in ovarian function remain unknown. If ovarian regression is mediated in a similar manner as testicular atrophy, short photoperiods may induce extensive apoptotic cell death in ovarian tissue.

Unlike the testes, where apoptosis in the reproducing adult is low (Young *et al.* 1999, 2001), high levels of apoptotic cell death are a fundamental component of normal adult ovarian function (Coucouvanis *et al.* 1993, Johnson 2003). Ultimately, the fate of over 99.9% of all oocytes is death via germ-cell attrition or follicular atresia (reviewed in Morita & Tilly 1999). In addition to germ-cell death prior to birth, follicular atresia is a normal part of each ovulatory cycle. Prior to ovulation, cohorts of follicles are recruited; however, only select follicles develop fully and ovulate. Morphologic assessments, along with *in situ* and gel electrophoresis analyses of DNA and apoptotic proteins, implicate apoptosis as the molecular mechanism underlying follicular atresia (Hughes & Gorospe 1991, Tilly *et al.* 1991, Palumbo & Yeh 1994). In addition to cell death during follicular development, apoptosis is also involved in regression of the corpus luteum at the end of the ovarian cycle (Zeleznick *et al.* 1989, Guo *et al.* 1998, Roughton *et al.* 1999). Among the proteins in the apoptotic cascade, active caspase-3 is consistently upregulated in granulosa cells of atretic follicles, and is considered an accurate marker of follicular apoptosis (Fenwick & Hurst 2002). Indeed, knockout studies confirm that caspase-3, an effector enzyme, is required for normal programmed cell death of granulosa cells in the ovary (Matikainen *et al.* 2001).

Despite the extensive research on the role of apoptosis in normal ovarian development and function, little is known about its role in the suppression of ovarian activity in seasonally breeding mammals, specifically Siberian hamsters. We hypothesized that exposing female Siberian hamsters to short (inhibitory) as opposed to long (control) photoperiods would result in early disruption of ovarian function mediated by apoptosis. In the present study, we investigated the progressive inhibitory effects of short photoperiods on Siberian hamster ovarian activity after 3, 6, 9 and 12 weeks of SD or LD exposure. Ovarian activity was determined through examination of ovarian morphology and assessing sex-steroid

concentrations. In addition, the mechanism of ovarian regression was investigated, as we hypothesized that exposure to short days would increase the extent of ovarian apoptosis above that observed in LD females. The extent of apoptosis in ovarian regression was determined by both TUNEL analysis and caspase-3 immunohistochemistry.

Materials and Methods

Animals and tissue processing

Female (n = 60) and male (n = 8) adult (60–90 days of age) Siberian hamsters were obtained from the colony of Dr Kathryn Wynne-Edwards, Queens University (Kingston, Ontario, Canada). All experiments were conducted at California State University, Long Beach (CSULB), in compliance with CSULB and NRC guidelines for use of laboratory animals. All animals were housed in individual polypropylene cages outfitted with bedding and had free access to food (a mixture of Lab Rodent Diet 5001 and Mazuri Hamster and Gerbil Diet, both from Purina, Brentwood, MO, USA) and tap water. Prior to the start of the experiment, all hamsters were acclimated to a 16-h light:8-h darkness (16L:8D), LD photoperiod for 2 weeks. Each female hamster was randomly assigned to housing in either LD (n = 20) or SD photoperiods (SD; 8L:16D; n = 40 to allow for potential nonresponders). In both rooms, the temperature was maintained at 20 ± 2 °C. Male hamsters (four in each room) were housed in separate cages (i.e. not in physical contact with females) and placed randomly among female hamsters to promote estrous cyclicity (Dodge *et al.* 2002b). Four days prior to tissue collection, male soil bedding was placed in female cages to synchronize female estrus cycles (Dodge *et al.* 2002b). Exposure to male bedding did not appear to disrupt ovarian regression in SD females, as response to photoperiod was significant across a number of measures. At weeks 3, 6, 9 and 12, SD (n = 10) and LD (n = 5) female hamsters were weighed and their estrus cycle was staged by vaginal cytology (Snell 1941). Cells were collected by inserting a cotton swab moistened with saline solution into the vagina and then smearing the cotton swab onto a microscope slide. The slides were then air-dried, stained with Fisher's Hema 3 Wright-Giesma solution (Fisher Scientific, Pittsburgh, PA, USA) and visualized under a light microscope. The following cellular characteristics were used to stage estrous cycles: estrus (many nonnucleated squamous cells, few endonucleated epithelial cells, no leukocytes), diestrus I (few nonnucleated squamous cells, many leukocytes), diestrus II (few endonucleated epithelial cells, many leukocytes) and proestrus (few nonnucleated epithelial cells, few leukocytes, many endonucleated epithelial cells). For a more accurate comparison among cycling individuals, tissues were collected from all hamsters only when their vaginal cytology revealed they were in diestrus II, as prolonged SD exposure induces vaginal cytology typical of this stage in photosensitive rodents (Beasley *et al.* 1981). If it was determined that a hamster was not in diestrus II, vaginal smears were conducted on subsequent days until diestrus II was reached; the maximal number of additional days was fewer than 3 for all weeks of tissue collection. Once confirmed to be in diestrus II, hamsters were injected intraperitoneally with a ketamine/xylazine cocktail at a dose of 200 mg/kg (ketamine) and 20 mg/kg (xylazine). Blood samples were collected by retro-orbital puncture with heparinized capillary tubes. Hamsters were killed by rapid cervical dislocation; ovaries and uteri were immediately removed, weighed and fixed in 10% neutral buffered formalin for 7 days. Contralateral organs were flash-frozen in liquid nitrogen for mRNA analysis. After fixation, tissues were processed through a series of PBS washes, dehydrated in a graded series of ethanol solutions and subsequently embedded in paraffin. Serial sections of 6 μm thickness were collected from every 60μm of tissue and mounted onto Superfrost-plus microscope slides (Fisher Scientific) for follicle counting, TUNEL and immunohistochemical analyses.

RIA

After blood collection, plasma was subsequently separated by centrifugation (1500 *g* for 5 min) and stored at −80 °C until RIA. Plasma estradiol and progesterone concentrations were determined with the Ultra-Sensitive estradiol RIA and progesterone RIA ^{125}I double-antibody kits (Diagnostic Systems Laboratories, Webster, TX, USA). All samples were assayed in duplicate, and their radioactivity was measured with a Perkin–Elmer Cobra II gamma counter (Packard Instruments, Boston, MA, USA). Values were entered into Sigma Plot software (SPSS Inc., Chicago, IL, USA), a standard curve was generated with the four-parameter logistic curve function, and the final hormone concentrations were calculated with the Sigma Plot standard curve analysis function. Assay standards and controls for both estradiol and progesterone were within the normal limits. The intra- and interassay coefficients of variation for estradiol were 6.3 and 4.7% respectively. For progesterone, they were 4.9 and 7.9% respectively. Estradiol concentration values were compared against those of the CSULB Endocrine Laboratory (Schmidt & Kelley 2001). The lower limits of detection for the estradiol and progesterone assays were 5 pg/ml and 0.1 ng/ml respectively, with low cross-reactions to other steroids: 0.64 – 2.40% and 0.88 – 5.0% respectively.

Follicle counting

The effect of inhibitory photoperiods on ovarian activity was assessed by histologic examination. Tissues were deparaffinized in xylene, rehydrated through a graded series of ethanols, washed in PBS and then stained with hematoxylin and eosin. A minimal number of sections that contained fewer than four ovarian structures were excluded from the assessment. Ovarian structures were grouped and counted according to the following classifications:

- preantral follicle (one or more layers of cuboidal granulosa cells, no antrum present)
- early antral/antral follicle (multiple layers of granulose cells, antrum present)
- atretic follicle (presence of at least five pyknotic granulosa cell nuclei and/or degrading oocyte)
- advanced atretic follicle (pockets of highly vascularized, luteinized cells surrounded by pseudotheca, diameter of 210–430 μm)
- terminal atretic follicle (pockets of highly vascularized, luteinized cells, diameter of 150–270μm (Knigge & Leathem 1956)
- corpora lutea.

Hamsters ($n = 3$) whose ovarian histology revealed corpora lutea after 12 weeks of SD exposure were identified as nonresponders and were eliminated from this study. To avoid double counting, only follicles with a visible oocyte were counted, or adjacent sections were considered when structures lacking oocytes, such as corpus luteum, were counted. An observer blind to photoperiod and weeks in treatment verified follicle counts. For each ovary, the average number of each ovarian structure per section was determined from the six sections counted per animal.

TUNEL assay

Apoptotic activity was assessed by the *in situ* terminal deoxynucleotidyl transferase (TdT)-mediated dUTP nick end-labeling (TUNEL) technique with the TACS 2TdT Blue Label kit (Trevigen, Gaithersburg, MD, USA). The experiment was conducted in accordance with the protocol supplied by the manufacture. Positive control sections were pretreated with TACS-Nuclease, to induce DNA fragmentation before the TUNEL reaction. Negative controls were processed in the absence of the TdT enzyme and showed no staining. After labeling, sections were examined with brightfield illumination. Follicles with at least five labeled cells were

considered TUNEL positive. For each ovary, the average number of TUNEL-positive follicles per section was determined from the six sections counted per animal.

Caspase-3 immunostaining

To assess apoptotic cell death further, the effector enzyme, active caspase-3, was analyzed by immunohistochemistry. For caspase-3 immunostaining, six representative ovarian tissue sections per animal were deparaffinized in xylene, rehydrated in ethanol solutions and rinsed in PBS. To facilitate antigen retrieval, sections were treated with Antigen Unmasking Solution (Vector Laboratories, Burlingame, CA, USA) and heated in a pressure cooker for 10 min. Endogenous peroxidases were quenched in a 3% H_2O_2/-methanol solution. After 40-min blocking with a 1:20 solution of normal goat serum to PBS/Tween 20, sections were incubated overnight at room temperature in a 1:125 dilution of anti-human/mouse active caspase-3 antibody (R&D Systems, Minneapolis, MN, USA). The sections were rinsed in PBS, and then incubated for 45 min at room temperature with a biotinylated goat anti-rabbit immunoglobulin G secondary antibody (1:200; Vector Laboratories). Immediately after incubation with the secondary antibody, sections were incubated for 30 min at room temperature with avidin-biotin-peroxidase solution (Vectastain elite ABC kit; Vector Laboratories). The antigen was visualized with the NovaRed Substrate kit (Vector Laboratories) and counterstained with hematoxylin. Negative control sections were processed in the absence of the active caspase-3 primary antibody and showed no staining. Follicles with at least five intensely labeled cells were considered active caspase-3 positive; diffuse staining was not quantified. For each ovary, the average number of active caspase-3-positive follicles per section was determined from the six sections counted.

Caspase-3 PCR analysis

In addition to caspase-3 immunolabeling, relative levels of caspase-3 mRNA were assessed in all hamsters. After all tissue collection, total RNA was isolated from the frozen contralateral ovaries with TRIzol reagent (Invitrogen) according to the Invitrogen standard protocol. For all samples that contained sufficient RNA (five week-12 SD samples were removed from further analysis due to inadequate concentrations of RNA), reverse transcription was carried out on 1 μg DNase (Promega)-treated RNA with Molony murine leukemia virus reverse transcriptase (Promega) and random hexamer primers for 2 h at 37 °C. For the semiquantitative PCR, primer concentration, cycle number and optimal temperature were determined empirically. Reactions were conducted at 94 °C for 30 s, annealing at 57 °C for 1 min, and extension at 72 °C for 1 min for 32 (caspase-3) or 25 (β-actin) cycles. Primer sequences for caspase-3 were as follows: forward, GGA-GCAGCTTTGTGTGTGTGATTC; reverse, TCCATCCTTTG-ACTCTGCTCATGG. Primer sequences for the internal standard, β-actin were as follows: forward, AGGGTGTG-ATGGTGGGAA; reverse, CATCTGCTGGAAGGTGGA. For each hamster, 10μl of PCR product was electrophoresed through a 2% agarose gel containing 1 μl ethidium bromide to allow visualization. Gels were visualized with the Gel Doc XR documentation system (BioRad, Hercules, CA, USA), and density of bands was analyzed with Quantity One software (Discovery Series, BioRad). For each hamster, the optical density of the caspase-3 band was normalized by division by density of the standard β-actin band to obtain the relative mRNA expression for caspase-3.

Statistical evaluation of data

All results are presented as the mean ± S.E.M. All data were analyzed by one-way ANOVA with the significance level set at 0.05, using the Prism 4 statistical software package (GraphPad Software, San Diego, CA, USA). In cases of unequal variances among groups, data were square-root transformed prior to ANOVA, with the exception of the atretic follicle count, which

was log transformed to normalize data. To isolate significant differences between groups, the Student–Newman–Keuls post-hoc test was used for all pairwise comparisons.

Results

No significant differences were observed among LD hamsters for any parameter ($P > 0.2$ in all cases, except for corpus luteum counts, in which $P > 0.08$); therefore, their data were pooled to create a single LD control group for comparison. For example, the following are *P* and mean values for ovary pair mass, estradiol concentrations, preantral follicle and TUNEL-positive follicle counts from hamsters exposed to LD for 3, 6, 9 and 12 weeks: ovary pair mass, $P = 0{:}87$ (week-3 mean = 0.024 mg, week-6 mean = 0.024 mg, week-9 mean = 0.020 mg, week-12 mean = 0.024 mg); estradiol concentrations, $P = 0.58$ (week-3 mean = 25.78 pg/ml, week-6 mean = 12.04 pg/ml, week-9 mean = 23.48 pg/ml, week-12 mean = 26.23 pg/ml); preantral follicles per section, $P = 0{:}99$ (week-3 mean = 3.61, week-6 mean = 3.54, week-9 mean = 3.46, week-12 mean = 3.38); number of TUNEL-positive follicles per ovarian section, $P = 0{:}74$ (week-3 mean = 0.823, week-6 mean = 1.10, week-9 mean = 1.21, week-12 mean = 0.873).

Body mass and reproductive organ masses

No significant difference existed between body masses of LD and SD hamsters despite an apparent trend toward a decreased body mass in SD hamsters ($P > 0.05$) (Table 1). Paired ovary mass declined twofold in SD hamsters by week 12 of photoperiod exposure compared with LD females ($P < 0.05$) (Table 1). A 1.4-fold reduction in uterine mass was first observed within 3 weeks of SD photoperiod treatment; by 12 weeks, continued SD exposure further reduced uterine mass by 3.5-fold as compared with LD controls ($P < 0.05$) (Table 1).

Hormone concentrations

Plasma estradiol concentrations decreased rapidly by 6 weeks of short as compared with long photoperiod exposure (Fig. 1). Within 9 weeks of SD exposure, estradiol concentrations were reduced 2.8- and 3.7-fold as compared with both LD and week-3 SD values respectively ($P < 0.05$). In contrast, no significant differences were noted in plasma progesterone concentrations between LD and SD females, or among the SD hamsters ($P > 0.05$ for all comparisons). Plasma progesterone concentrations averaged 3.27 (±0.5) ng/ml for LD females; 2.80 (±0.7) ng/ml for week-3 SD females; 2.69 (±0.9) ng/ml for week-6 SD females; 3.07 (±0.6) ng/ml for week-9 SD females; and 1.69 (±0.7) ng/ml for week-12 SD females.

Ovarian histology

Substantial histologic changes in Siberian hamster ovaries occurred in response to short photoperiod (Fig. 2). Ovaries from hamsters maintained under LD were typical of normal folliculogenesis and were characterized by the presence of follicles in all stages of development, atretic follicles and corpora lutea (Fig. 2A). Ovaries from hamsters exposed to 3 weeks of SD were also characterized by the presence of various types of follicles and corpora lutea; however, they also displayed increased numbers of atretic and advanced atretic follicles (Fig. 2B). Six weeks of SD exposure continued to promote the formation of advanced atretic follicles (Fig. 2C). By 9 weeks of SD exposure, advanced atretic follicles appeared to be in transition to terminal-stage atretic follicles (Fig. 2D). By week 12, SD ovaries were highly regressed, contained few follicles and no corpora lutea, and consisted mainly of terminal-stage atretic follicles (Fig. 2E).

Follicle counts

To determine the effects of short photoperiod on folliculogenesis and atresia, the number of preantral, early antral/antral, corpora lutea, atretic follicles, advanced atretic follicles, and

terminal-stage atretic follicles in week-3, -6, -9 and -12 SD ovaries were counted and compared with LD controls. When compared with LD ovaries, the number of preantral follicles in week-3, -6, and -9 SD ovaries remained constant (Table 2). However, the number of preantral follicles decreased at least 1.5-fold at week 12 when compared with LD and week-3 and -6 SD ovaries ($P < 0.05$). The number of early antral/antral follicles in week-3, -6 and -9 SD ovaries was consistent with the number in LD ovaries (Table 2). In contrast, at week 12, no early antral/antral follicles were observed in any week-12 SD ovaries, making this group significantly reduced as compared with all other groups ($P < 0.05$). The number of corpora lutea dropped rapidly (1.8-fold) with 3 weeks of short photoperiod treatment when compared with LD controls ($P < 0.05$) (Table 2). In SD hamsters, the number of corpora lutea remained low, but steady through weeks 6 and 9 and then declined to zero at week 12, a significant reduction as compared all groups ($P < 0.05$) (Table 2).

Atretic or degrading follicles were observed in all groups, as expected; however, numbers were significantly higher in the week-3 SD exposure group than in both LD and week-12 SD females ($P < 0.05$) (Fig. 3A). Short photoperiods induced the formation of advanced atretic and, subsequently, terminal atretic follicles in Siberian hamster ovaries (Fig. 3B and C). Exposure to short photoperiod caused a 1.7-fold increase in the number of advanced atretic follicles at week 3 compared with LD and all other SD groups ($P < 0.05$) (Fig. 3B). After this initial increase, a steady decline in the number of advanced atretic follicles was observed throughout the duration of the experiment. Terminal atretic follicles were first observed at 9 weeks of SD treatment (Fig. 3C). The number of terminal atretic follicles increased 3.4-fold in week-12 SD ovaries as compared with week-9 SD ovaries ($P < 0.001$). These structures were not identified in any LD, or week-3 or -6 SD ovaries.

TUNEL staining

In situ TUNEL analysis was used to detect the presence of apoptotic activity in ovarian sections (Fig. 4). As expected, healthy follicles showed low or no staining (Fig. 4A), whereas atretic follicles stained TUNEL positive in both LD and SD hamsters (Fig. 4B). TUNEL staining was predominately localized in granulosa cells of late preantral and early antral/antral follicles; no staining was detected in the thecal layer or stroma (Fig. 4B). Advanced atretic follicles exhibited low staining (<5 labeled cells), whereas no staining was observed in terminal atretic follicles (data not shown). No staining was detected in control sections processed without TdT enzyme (Fig. 4B inset). When quantified, ovaries from hamsters exposed to 3 weeks of SD had a 1.9-fold higher number of TUNEL-positive follicles per cross section than LD ovaries ($P < 0.01$) (Fig. 4C). This initial peak in apoptosis was followed by a steady decline in the number of TUNEL-positive follicles. By 12 weeks of SD exposure, the number of TUNEL-positive follicles was 2.4-fold lower than week-3 SD values ($P < 0.05$) (Fig. 4C) and was similar to that of LD controls.

Active caspase-3 protein immunolabeling

Immunohistochemistry was used to determine the level of active, proapoptotic caspase-3 protein expression in ovarian sections. Healthy follicles showed low or no active caspase-3 staining (Fig. 5A). Immunolabeling of active caspase-3 was confined to granulosa cells; no staining was noted in the thecal layer or stroma (Fig. 5B). Intense perinuclear staining was observed in degrading follicles, found predominately in week-3 SD ovaries and to a lesser extent in LD ovaries (Fig. 5B and C). In contrast, diffuse staining was typical of advanced and terminal atretic follicles, the prominent structures in week-9 and -12 SD ovaries (data not shown). No staining was observed in sections processed without primary antibody (Fig. 5B inset). When quantified, the number of active caspase-3 follicles with intense immunostaining per ovarian cross section increased 1.8-fold with 3 weeks of SD exposure as compared with

LD levels ($P < 0.05$) (Fig. 5C). The number of immunolabeled follicles then fell back to LD levels, and remained low through week-12 SD (Fig. 5C).

Ovarian expression of caspase-3 mRNA

Caspase-3 mRNA was detectable in hamster ovarian tissue in all groups, regardless of photoperiod exposure (Fig. 6A). After quantification of band density, relative expression of caspase-3 increased 1.3-fold in week-3 SD females as compared with LD and week-6 and -9 SD hamsters ($P < 0.05$) (Fig. 6B).

Discussion

Results from the present study demonstrate that, in Siberian hamsters, short photoperiods induce marked changes in ovarian mass, folliculogenesis and plasma estradiol concentrations, as compared with control hamsters exposed to long photoperiods. In addition, this is the first investigation of apoptosis during short photoperiod-induced ovarian regression: SD exposure increased levels of both TUNEL-positive cells and active caspase-3 mRNA/protein expression above quantities observed in LD females.

A rapid increase in follicular death, as determined by TUNEL staining and active caspase-3 immunolabeling/mRNA expression, was observed in SD ovaries within 3 weeks of SD exposure. These findings all corroborate a relatively rapid induction of increased ovarian apoptotic cell death, and implicate apoptosis as an initial process in SD-induced ovarian regression. Our observations in the female Siberian hamster are consistent with those in the male Siberian hamster, in which testicular apoptosis is significantly elevated during the first 3 weeks of SD exposure (Furuta *et al.* 1994).

The general pattern of caspase-3 mRNA expression levels mirrored that of active caspase-3 immunostaining; however, week-3 SD caspase-3 mRNA expression was not significantly higher than levels observed in week-12 SD individuals. This discrepancy is probably due to the reduced number of samples available for RNA analysis in the week-12 SD group. Ovaries from this group were extremely small, and we were not able to extract sufficient quantities of mRNA from five of these ovaries. The samples that were successfully processed represented the larger ovaries from that week; therefore, caspase-3 may still be upregulated slightly in this modified group.

The early onset of follicular apoptosis observed in the present study occurs in the absence of a decline in diestrus II estradiol concentrations; significant reductions in estradiol concentrations were not detected until week 9 of SD exposure. Therefore, estradiol withdrawal does not appear to be an initiating factor in SD-induced apoptotic activity. Instead, declines in circulating FSH are probably responsible for this early onset of gonadal apoptosis. In both peripubertal and adult male Siberian hamsters, a significant decline in plasma FSH is observed within 7 days of short photoperiod exposure (Yellon & Goldman 1987, Furtua *et al.* 1994). Furthermore, reductions in FSH concentrations are immediately followed by increases in testicular apoptotic DNA fragmentation in peripubertal male Siberian hamsters (Furtua *et al.* 1994). Although the first significant drop in FSH reportedly occurs at 6-week SD exposure in female Siberian hamsters (Schlatt *et al.* 1993), evidence suggests that even slight declines in FSH may be sufficient to induce follicular cell death (Uilenbroek *et al.* 1980). Alternatively, additional factors may trigger SD-induced gonadal apoptosis. LH acts a survival factor, particularly for preovulatory follicles (Braw & Tsafriri 1980); however, SD exposure reduces serum concentrations of LH in female Siberian hamsters (Dodge & Badura 2002a). In female Syrian hamsters (*Mesocricetus aureus*), SD exposure reduces circulating concentrations of IGF-I, which is also a survival factor in the ovary (Vaughan *et al.* 1994, Chun *et al.* 1996, Hsueh *et al.* 1996).

Analysis of ovarian histology revealed that short photoperiods had a detrimental effect on folliculogenesis. By 12 weeks of SD exposure, the number of preantral follicles declined significantly, which is consistent with the observation that most TUNEL-positive follicles are late preantral follicles. The number of early antral/antral follicles in ovaries from hamsters exposed to 3, 6 and 9 weeks of SD lengths was consistent with that observed in LD ovaries. Interestingly, despite the presence of early antral/antral follicles in hamsters exposed to 6 and 9 weeks of SD lengths, plasma concentrations of estradiol, predominately synthesized and secreted from early antral/antral follicles, were reduced. This suggests that the steroidogenic pathway was impaired in early antral/antral follicles present in week-6 and -9 SD ovaries, despite not appearing atretic or labeling positively for either TUNEL or active caspase-3.

In contrast to the significant decrease in estradiol concentrations between LD and SD hamsters, no significant differences in plasma progesterone concentrations were noted between the photoperiod groups. It is possible that the lack of difference in progesterone concentrations can be attributed to diestrus II-specific tissue collection, as progesterone concentrations are low at this point in the estrous cycle (Wynne-Edwards *et al.* 1987, Reburn *et al.* 1996). Diestrus II was selected since the vaginal cytology of acyclic photoperiod-sensitive rodents exposed to prolonged SD lengths is characteristic of diestrus II (Beasley *et al.* 1981). Had tissues been collected on diestrus I, when progesterone reaches a maximum, differences in plasma progesterone concentrations may have been observed between basal SD and peak LD concentrations. It is also possible that the hypertrophied granulosa cells from both advanced and terminal atretic follicles present in SD ovaries were secreting progesterone at concentrations equal to that produced by corpora lutea in LD ovaries. *In vitro* studies using antral follicles from golden hamsters (*Mesocricetus auratus*) suggest that steroidogenesis switches from estradiol to progesterone when follicular atresia is induced (Terranova 1981), and terminal atretic follicles in photoregressed Siberian hamsters are reported to be steroidogenic (van den Hurk *et al.* 2002).

It is well known that the uterus is a major target of estradiol and that estradiol is essential in maintaining uterine function (Clarke & Sutherland 1990). Indeed, withdrawal of estradiol via ovariectomy (West *et al.* 1978) or administration of antiestrogen agents (Luo *et al.* 1997) results in uterine atrophy. Interestingly, the first significant decline in uterine mass in the present study occurred at 3 weeks of SD exposure, when diestrus II estradiol concentrations were still elevated and comparable to those of LD hamsters. It is likely that the significant decline in uterine mass in the presence of normal estradiol concentrations is due to a decline in the number of estradiol receptors or alterations in estrogen receptor coregulatory proteins (Horwitz *et al.* 1996). Alterations in coregulatory protein expression have been associated with several physiologic events, including cancer (Anzick *et al.* 1997, Carroll *et al.* 2000) and initiation of parturition (Condon *et al.* 2003). Alternatively, it is possible that uterine atrophy in the presence of normal diestrus II estradiol concentrations may be the consequence of declines in estradiol concentrations on other days of the estrous cycle.

Ovaries from hamsters maintained under short photoperiods are characterized by the presence of increased numbers of advanced and terminal atretic follicles, structures that are typical of photoregressed hamsters (‘luteinized atretic follicles’ (van den Hurk *et al.* 2002)). While the exact origin and nature of advanced and terminal atretic follicles are unknown, they probably arise from former atretic follicles (Knigge & Leathem 1956). Advanced atretic follicles typically contain fewer than five TUNEL-positive cells and few cells exhibiting caspase-3 immunolabeling. These observations suggest that advanced atretic follicles are follicles near the completion of atresia. In the natural estrus cycle of mice, high caspase-3 staining is reported in the late stages of follicular atresia (Fenwick & Hurst 2002); however, to our knowledge, no structures similar to the advanced/terminal atretic follicles found in regressed hamster ovaries have been noted in mice. In the present study, the number of advanced atretic follicles declined

in hamsters exposed to SD, while there were concomitant increases in the number of terminal atretic follicles. In general, terminal atretic follicles exhibited no TUNEL labeling and only diffuse cytoplasmic active caspase-3 immunostaining, a fact which may imply that these structures are no longer undergoing apoptosis. The follicle counts, TUNEL and caspase-3 labeling patterns, and caspase-3 mRNA expression strongly suggest that SD exposure induces degrading or atretic follicles that give rise to advanced atretic follicles, which in turn give rise to terminal atretic follicles. Ovaries from hamsters exposed to LD contained advanced atretic follicles, albeit at significantly lower numbers than their SD counterparts, implying that advanced atretic follicles are part of normal follicular atresia. However, no terminal atretic follicles were observed in LD ovaries, suggesting that under the influence of short photoperiods, the normal follicular atresia pathway is altered.

Taken together, data from the present study suggest that 3-week SD exposure induces increases in apoptotic activity, which in turn effectively initiates a decline in ovarian function, as evident by declines in estradiol secretion, number of follicles and ovulation events in subsequent weeks. Indeed, future studies examining ovarian apoptotic activity during weeks 0–3 of SD exposure are warranted to define the precise moment when ovarian demise begins. In addition, studies are necessary to determine the cellular and hormonal properties of terminal atretic follicles in order to elucidate the possible role of these structures in ovaries of hamsters exposed to short photoperiods. Furthermore, studies are needed to determine how the ovary regains function during spontaneous recrudescence.

Acknowledgements

We thank Dr Greg Demas and his laboratory at Indiana University for generous donation of pilot tissue; Drs Tom Douglass, Mason Zhang and Dessie Underwood for use of their equipment and technical expertise; Jesus Reyes for his assistance with the RIA; and, finally, our CSULB Reproductive Laboratory colleagues for their advice, particularly Coventry Dougherty and Luwanda Jenkins for their aid with histology techniques, Hsin-Jan Peng and Fatemeh Moemenbellahfard for help with tissue collection, and Trevor Salverson for preparing cDNA. This project was supported by HHMI grant no. 52002663 (C S M), a Howell/CSUPERB Research Fellowship (C S M), NIH SCORE grant no. 2506GM06119-05 (K A Y), and a CSULB SCAC grant (K A Y). The authors declare that there is no conflict of interest that would prejudice the impartiality of this scientific work.

References

Anzick SL, Kononen J, Walker RL, Azorsa DO, Tanner MM, Guan XY, Sauter G, Kallioniemi OP, Trent JM, Meltzer PS. AIB1, a steroid receptor coactivator amplified in breast and ovarian cancer. Science 1997;277:965–968. [PubMed: 9252329]

Beasley LJ, Johnston PG, Zucker I. Photoperiodic regulation of reproduction in postpartum *Peromyscus leucopus*. Biology of Reproduction 1981;24:962–966. [PubMed: 7272403]

Bergmann M. Photoperiod and testicular function in *Phodopus sungorus*. Advances in Anatomy, Embryology, and Cell Biology 1987;105:1–76.

Braw RH, Tsafiri A. Follicles explanted from pentobarbitone-treated rats provide a model for atresia. Journal of Reproduction and Fertility 1980;59:259–265. [PubMed: 7431284]

Bronson, FH. Mammalian Reproductive Biology. Chicago: University of Chicago Press; 1989.

Buchanan KL, Yellon SM. Delayed puberty in the male Djungarian hamster: effect of short photoperiod or melatonin treatment on the GnRH neuronal system. Neuroendocrinology 1991;54:96–102. [PubMed: 1766555]

Carroll RS, Brown M, Zhang J, DiRenzo J, De Mora JF, Black PM. Expression of a subset of steroid receptor cofactors is associated with progesterone receptor expression in meningiomas. Clinical Cancer Research 2000;6:3570–3575. [PubMed: 10999746]

Chun SY, Billig H, Tilly JL, Furuta I, Tsafriri A, Hsueh AJ. Gonadotropin suppression of apoptosis in cultured preovulatory follicles: mediatory role of endogenous insulin-like growth factor 1. Endocrinology 1994;135:1845–1853. [PubMed: 7525255]

Clarke CL, Sutherland RL. Progestin regulation of cellular proliferation. Endocrine Reviews 1990;11:266–301. [PubMed: 2114281]

Condon JC, Jeyasuria P, Faust JM, Wilson JW, Mendelson CR. A decline in the levels of progesterone receptor coactivators in the pregnant uterus at term may antagonize progesterone receptor function and contribute to the initiation of parturition. PNAS 2003;100:9518–9523. [PubMed: 12886011]

Coucouvanis EC, Sherwood SW, Carswell-Crumpton C, Spack EG, Jones PP. Evidence that the mechanism of prenatal germ cell death in the mouse is apoptosis. Experimental Cell Research 1993;209:238–247. [PubMed: 8262141]

Dodge JC, Badura LL. 5HT and 5HIAA dialysate levels within the arcuate nucleus of the hypothalamus: relationship with photoperiod-driven differences in serum prolactin and luteinizing hormone in the Siberian hamster. Brain Research 2002a;946:171–178. [PubMed: 12137919]

Dodge JC, Kristal MB, Badura LL. Male-induced estrus synchronization in the female Siberian hamster (*Phodopus sungorus sungorus*). Physiological Behaviour 2002b;77:227–231.

Fenwick MA, Hurst PR. Immunohistochemical localization of active caspase-3 in the mouse ovary: growth and atresia of small follicles. Reproduction 2002;124:659–665. [PubMed: 12417004]

Furuta I, Porkka-Heiskanen T, Scarbrough K, Tapanainen J, Turek FW, Hsueh AJ. Photoperiod regulates testis cell apoptosis in Djungarian hamsters. Biology of Reproduction 1994;51:1315–1321. [PubMed: 7888511]

Glass JD. Short photoperiod-induced gonadal regression: effects on the gonadotropin-releasing hormone (GnRH) neuronal system of the white-footed mouse, *Peromyscus leucopus*. Biology of Reproduction 1986;35:733–743. [PubMed: 3539214]

Guo K, Wolf V, Dharmarajan AM, Feng Z, Bielke W, Saurer S, Friis R. Apoptosis-associated gene expression in the corpus luteum of the rat. Biology of Reproduction 1998;58:739–746. [PubMed: 9510961]

Hoffmann K. Photoperiod, pineal, melatonin and reproduction in hamsters. Progress in Brain Research 1979;52:397–415. [PubMed: 575802]

Hoffmann K, Illnerova H. Photoperiodic effects in the Djungarian hamster. Rate of testicular regression and extension of pineal melatonin pattern depend on the way of change from long to short photoperiods. Neuroendocrinology 1986;43:317–321. [PubMed: 3736780]

Horwitz KB, Jackson TA, Bain DL, Richer JK, Takimoto GS, Tung L. Nuclear receptor coactivators and corepressors. Molecular Endocrinology 1996;10:1167–1177. [PubMed: 9121485]

Hsueh AJ, Eisenhauer K, Chun SY, Hsu SY, Billig H. Gonadal cell apoptosis. Recent Progress in Hormone Research 1996;51:433–455. [PubMed: 8701090]discussion 455–456

Hughes FM Jr, Gorospe WC. Biochemical identification of apoptosis (programmed cell death) in granulosa cells: evidence for a potential mechanism underlying follicular atresia. Endocrinology 1991;129:2415–2422. [PubMed: 1935775]

Johnson AL. Intracellular mechanisms regulating cell survival in ovarian follicles. Animal Reproduction Science 2003;78:185–201. [PubMed: 12818644]

Knigge KM, Leathem JH. Growth and atresia of follicles in the ovary of the hamster. Anatomy Records 1956;124:679–707.

Knopper LD, Boily P. The energy budget of captive Siberian hamsters, *Phodopus sungorus*, exposed to photoperiod changes: mass loss is caused by a voluntary decrease in food intake. Physiological and Biochemical Zoology 2000;73:517–522. [PubMed: 11009406]

Luo S, Martel C, Sourla A, Gauthier S, Mâerand Y, Belanger A, Labrie C, Labrie F. Comparative effects of 28-day treatment with the new anti-estrogen EM-800 and tamoxifen on estrogen-sensitive parameters in intact mice. International Journal of Cancer 1997;73:381–391.

Matikainen T, Perez GI, Zheng TS, Kluzak TR, Rueda BR, Flavell RA, Tilly JL. Caspase-3 gene knockout defines cell lineage specificity for programmed cell death signaling in the ovary. Endocrinology 2001;142:2468–2480. [PubMed: 11356696]

Morita Y, Tilly JL. Oocyte apoptosis: like sand through an hourglass. Developmental Biology 1999;213:1–17. [PubMed: 10452843]

Ohno S, Smith JB. Role of fetal follicular cells in meiosis of mammalian oocytes. Cytogenetics 1964;13:324–333. [PubMed: 14252175]

Palumbo A, Yeh J. In situ localization of apoptosis in the rat ovary during follicular atresia. Biology of Reproduction 1994;51:888–895. [PubMed: 7531507]

Prendergast BJ, Nelson RJ. Spontaneous 'regression' of enhanced immune function in a photoperiodic rodent *Peromyscus maniculatus*. Proceedings in Biological Science 2001;268:2221–2228.

Pyter LM, Hotchkiss AK, Nelson RJ. Photoperiod-induced differential expression of angiogenesis genes in testes of adult *Peromyscus leucopus*. Reproduction 2005;129:201–209. [PubMed: 15695614]

Reburn CJ, Wynne-Edwards KE. Novel patterns of progesterone and prolactin in plasma during the estrous cycle in the Djungarian hamster (*Phodopus campbelli*) as determined by repeated sampling of individual females. Biology of Reproduction 1996;54:819–825. [PubMed: 8924501]

Roughton SA, Lareu RR, Bittles AH, Dharmarajan AM. Fas and Fas ligand messenger ribonucleic acid and protein expression in the rat corpus luteum during apoptosis-mediated luteolysis. Biology of Reproduction 1999;60:797–804. [PubMed: 10084951]

Schlatt S, Niklowitz P, Hoffmann K, Nieschlag E. Influence of short photoperiods on reproductive organs and estrous cycles of normal and pinealectomized female Djungarian hamsters, *Phodopus sungorus*. Biology of Reproduction 1993;49:243–250. [PubMed: 8373948]

Schmidt KE, Kelley KM. Down-regulation in the insulin-like growth factor (IGF) axis during hibernation in the golden-mantled ground squirrel, *Spermophilus lateralis*: IGF-I and the IGF-binding proteins (IGFBPs). Journal of Experimental Zoology 2001;289:66–73. [PubMed: 11169494]

Snell, G. Biology of the Laboratory Mouse. New York: Dover Publications; 1941. p. 55-88.

Terranova PF. Steroidogenesis in experimentally induced atretic follicles of the hamster: a shift from estradiol to progesterone synthesis. Endocrinology 1981;108:1885–1890. [PubMed: 7215305]

Tilly JL, Kowalski KI, Johnson AL, Hsueh AJ. Involvement of apoptosis in ovarian follicular atresia and postovulatory regression. Endocrinology 1991;129:2799–2801. [PubMed: 1718732]

Uilenbroek JT, Woutersen PJ, van der Schoot P. Atresia of preovulatory follicles: gonadotropin binding and steroidogenic activity. Biology of Reproduction 1980;23:219–229. [PubMed: 6774780]

van den Hurk R, Dijkstra G, De Jong FH. Enhanced serum oestrogen levels and highly steroidogenic, luteinized atretic follicles in the ovaries of the Djungarian hamster (*Phodopus sungorus*) kept under a short photoperiod from birth. European Journal of Endocrinology 2002;147:701–710. [PubMed: 12444903]

Vaughan MK, Buzzell GR, Hoffman RA, Menendez-Pelaez A, Reiter RJ. Insulin-like growth factor-1 in Syrian hamsters: interactions of photoperiod, gonadal steroids, pinealectomy, and continuous melatonin treatment. Proceedings of the Society of Experimental Biology and Medicine 1994;205:327–331.

Vaux DL, Strasser A. The molecular biology of apoptosis. PNAS 1996;93:2239–2244. [PubMed: 8637856]

West NB, Norman RL, Sandow BA, Brenner RM. Hormonal control of nuclear estradiol receptor content and the luminal epithelium in the uterus of the golden hamster. Endocrinology 1978;103:1732–1741. [PubMed: 748013]

Wynne-Edwards KE, Terranova PF, Lisk RD. Cyclic Djungarian hamsters, *Phodopus campbelli*, lack the progesterone surge normally associated with ovulation and behavioral receptivity. Endocrinology 1987;120:1308–1316. [PubMed: 3830052]

Yellon SM, Goldman BD. Influence of short days on diurnal patterns of serum gonadotrophins and prolactin concentrations in the male Djungarian hamster, *Phodopus sungorus*. Journal of Reproduction and Fertility 1987;80:167–174. [PubMed: 3110410]

Young KA, Nelson RJ. Short photoperiods reduce vascular endothelial growth factor in the testes of Peromysius leucopus. American Journal of Physiology–Regulatory, Integrative and Comparative Physiology 2000;279:1132–1137.

Young KA, Nelson RJ. Mediation of seasonal testicular regression by apoptosis. Reproduction 2001;122:677–685. [PubMed: 11690527]

Young KA, Zirkin BR, Nelson RJ. Short photoperiods evoke testicular apoptosis in white-footed mice (*Peromyscus leucopus*). Endocrinology 1999;140:3133–3139. [PubMed: 10385406]

Young KA, Zirkin BR, Nelson RJ. Testicular apoptosis is down-regulated during spontaneous recrudescence in white-footed mice (*Peromyscus leucopus*). Journal of Biological Rhythms 2001;16:479–488. [PubMed: 11669421]

Zeleznick AJ, Ihrig LL, Bassett SG. Developmental expression of Ca^{++}/Mg^{++}-dependent endonuclease activity in rat granulose and luteal cells. Endocrinology 1989;125:2218–2220. [PubMed: 2791987]

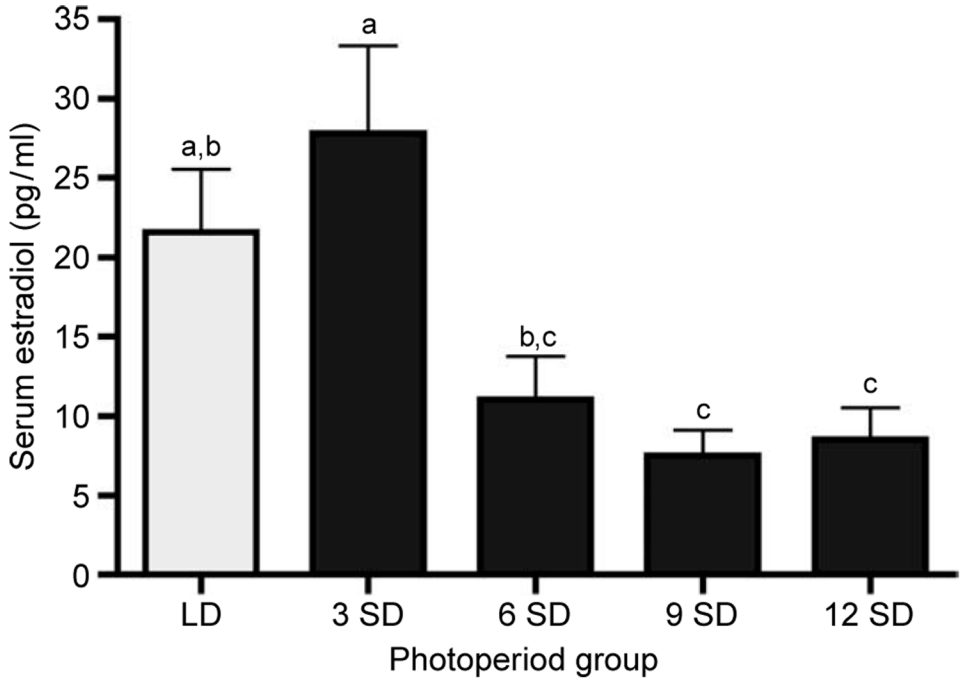

Figure 1.
Plasma concentrations (mean ± S.E.M.) of estradiol in Siberian hamsters exposed to long (LD, clear bars; 16L:8D) and short (SD, solid bars; 8L:16D) photoperiods. Groups with different letters are significantly different ($P<0.05$).

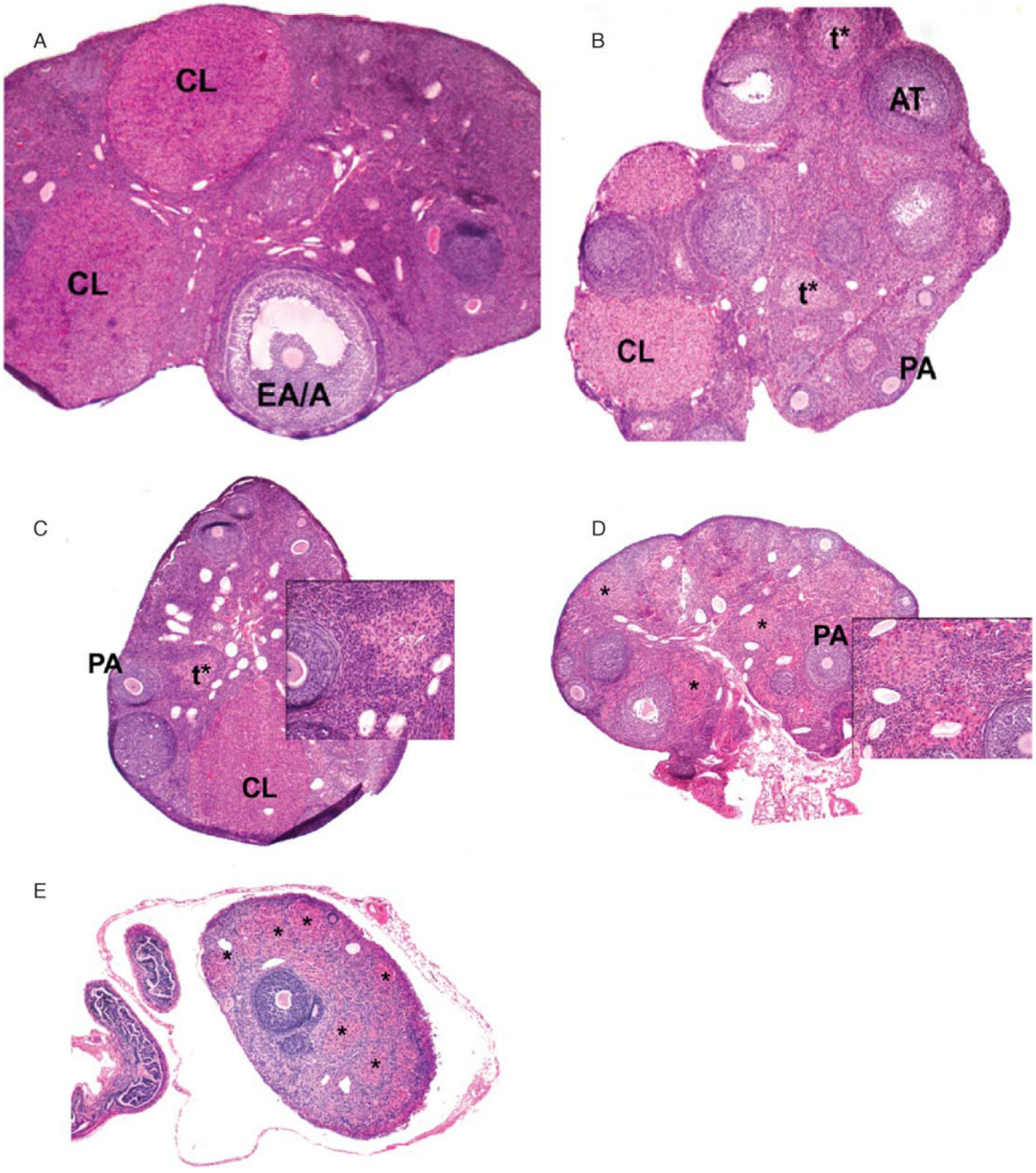

Figure 2.

Hematoxylin and eosin staining of ovary cross sections from Siberian hamsters maintained under long photoperiods (A) or short photoperiods for 3, 6, 9 and 12 weeks (B–E respectively). PA: preantral follicle; EA/A, early antral/antral follicle; AT, atretic follicle; CL, corpus luteum; t*, advanced atretic follicle; *, terminal atretic follicle. × 4 for A–E; × 20 for insets C and D.

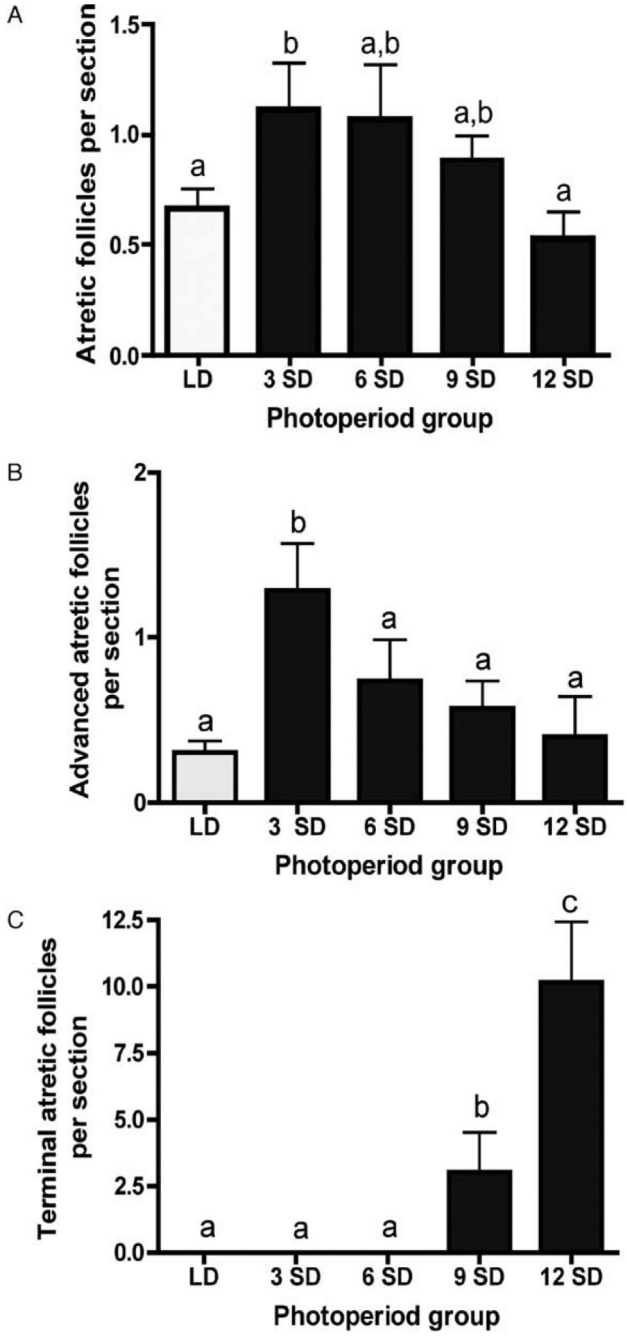

Figure 3.

Mean ± S.E.M. number of atretic (A), advanced atretic (B) and terminal atretic (C) follicles in Siberian hamsters housed in long (LD, clear bars) and short (SD, solid bars) photoperiods. Groups with different letters are significantly different ($P < 0.05$).

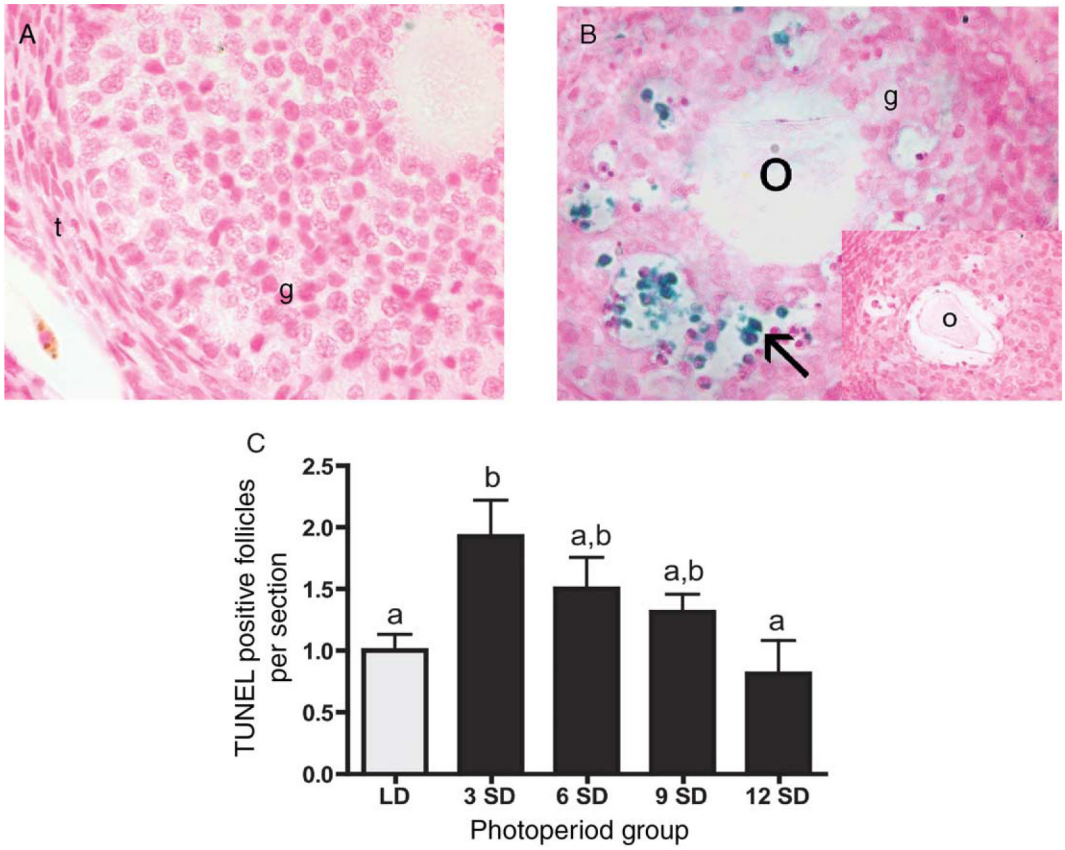

Figure 4.

Representative cross sections from ovaries from Siberian hamsters maintained in (A) long days and (B) 3 weeks of short days. These sections illustrate the typical low staining in healthy follicles (A) and high levels of TUNEL staining in atretic follicles (B). No staining was evident in control sections processed without TdT enzyme (B inset depicts control atretic follicle). Arrow indicates TUNEL-positive cells. O: oocyte; t: thecal layer; g: granulosa cells. × 40 for A, B, inset. (C) Quantification of number of TUNEL-positive follicles per ovarian cross section (mean ± S.E.M.) in Siberian hamsters housed in long (LD, clear bars) and short (SD, solid bars) photoperiods. Groups with different letters are significantly different ($P < 0.05$).

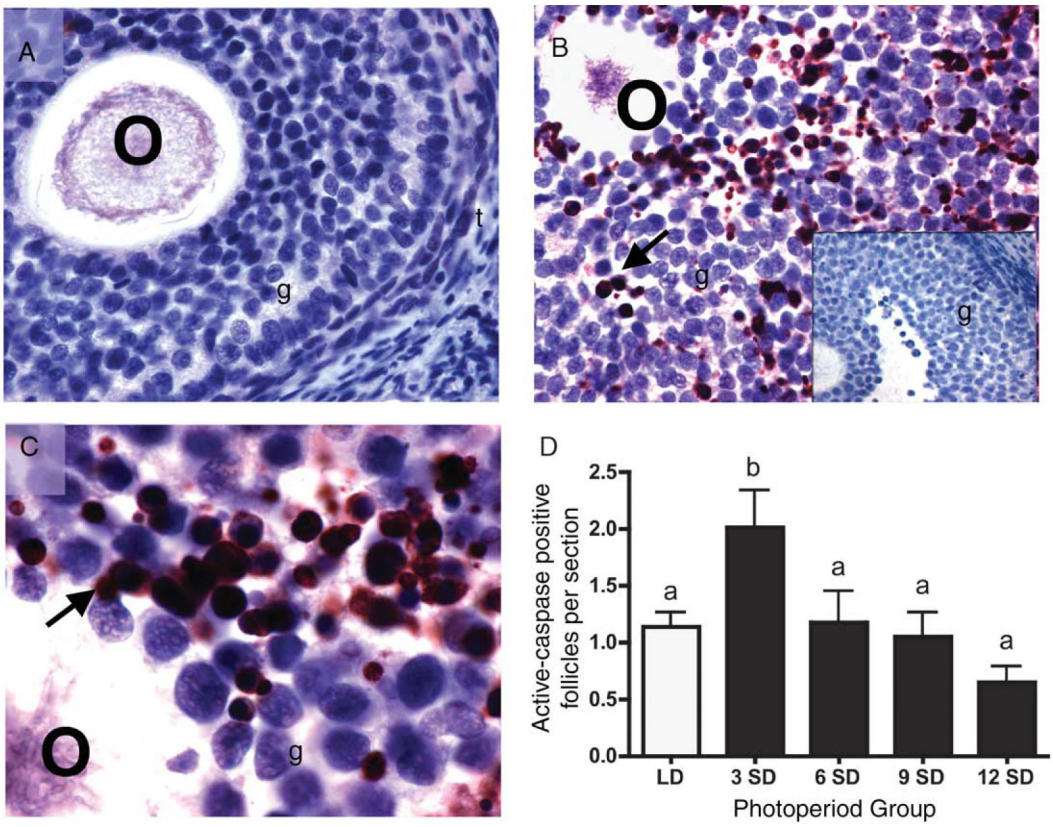

Figure 5.

Representative cross sections from ovaries of Siberian hamsters maintained in LD (A) or 3 weeks of SD (B and C). These sections illustrate the typical lack of active caspase-3 staining in healthy follicles (A), and intense active caspase-3 immunostaining in atretic follicles (B and C). No staining was evident in sections processed without primary antibodies (B inset depicts control atretic follicle). Arrows indicate intense immunolabeling for active caspase-3. O, oocyte; t: thecal layer; g, granulosa cells. × 40 for A, B and B inset; × 100 for C. (D) Quantification of active-caspase-3 positive follicles per ovarian cross section (mean + S.E.M.) in Siberian hamsters housed in long (LD, clear bars; 16L:8D) and short (SD, solid bars; 8L: 16D) photoperiods. Groups with different letters are significantly different ($P < 0.05$).

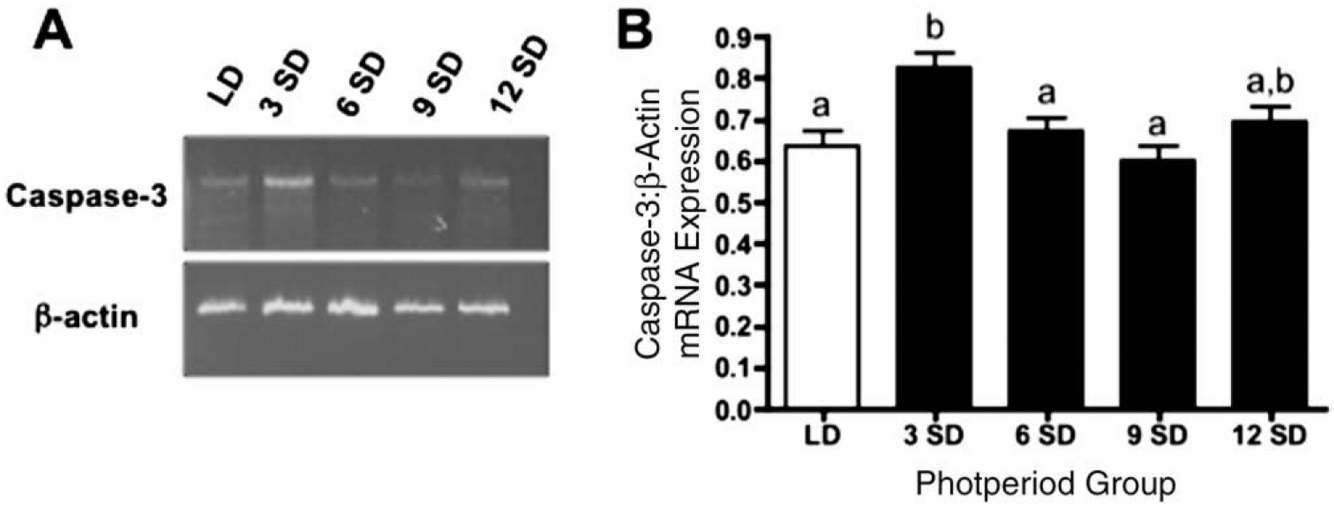

Figure 6.

Representative RT–PCR data for caspase-3/β actin expression for Siberian hamsters housed in LD, or 3, 6, 9 or 12 weeks in SD (A). Mean density ± S.E.M. of caspase-3 mRNA expression normalized to β-actin expression in Siberian hamsters housed in long (LD, clear bars) and short (SD, solid bars) photoperiods (B). Groups with different letters are significantly different ($P < 0.05$).

Table 1

Effects of long (16L:8D) vs short (8L:16D) photoperiod exposure on body mass, ovary pair mass and uterine mass of Siberian hamsters.

Photoperiod group	Body mass (g)*	Paired ovary mass (mg)*	Uterine mass (mg)*
LD	32.42 ± 1.28	23.0 ± 1.9^{a}	128.5 ± 10.0^{a}
3 SD	33.10 ± 1.17	22.0 ± 3.6^{a}	90.0 ± 7.1^{b}
6 SD	32.60 ± 2.47	17.0 ± 3.0^{a}	91.0 ± 14.9^{b}
9 SD	28.70 ± 1.62	17.0 ± 1.5^{a}	77.4 ± 12.8^{b}
12 SD	27.19 ± 1.02	11.4 ± 2.4^{b}	37.1 ± 9.2^{c}

*Values represent the mean ± S.E.M

^{a,b,c}Within each column, values with different letters differ significantly ($P < 0.05$).

Table 2

Effects of long (16L: 8D) vs short (8L:16D) photoperiod exposure on preantral follicles, early antral/antral follicles and corpora lutea in Siberian hamsters.

Photoperiod group	Preantral*	Early antral/antral*	Corpora lutea†
LD	3.50 ± 0.28^{a}	0.310 ± 0.052^{a}	3.25 ± 0.31^{a}
3 SD	3.65 ± 0.31^{a}	0.339 ± 0.091^{a}	1.80 ± 0.51^{a,b}
6 SD	3.68 ± 0.31^{a}	0.338 ± 0.080^{a}	1.90 ± 0.55^{a,b}
9 SD	2.92 ± 0.32^{a,b}	0.333 ± 0.081^{a}	1.89 ± 0.45^{a,b}
12 SD	2.15 ± 0.40^{b,c}	0.000 ± 0.000^{b}	0.00 ± 0.00^{c}

*Values represent the mean ± S.E.M. pre ovarian section

†Values represent the mean ± S.E.M. per ovary.

^{a,b,c}Within each column, values with different letters differ significantly ($P < 0.05$).